MOLECULAR AND CELLULAR BIOLOGY, Mar. 2008, p. 1688–1701 Vol. 28, No. 5
0270-7306/08/$08.00+0 doi:10.1128/MCB.01154-06

Mice Lacking Histone Deacetylase 6 Have Hyperacetylated Tubulin but Are Viable and Develop Normally▽†

Yu Zhang,[1]‡ SoHee Kwon,[1] Teppei Yamaguchi,[1] Fabien Cubizolles,[1] Sophie Rousseaux,[2] Michaela Kneissel,[3] Chun Cao,[1] Na Li,[1] Hwei-Ling Cheng,[4] Katrin Chua,[4] David Lombard,[4] Adam Mizeracki,[1] Gabriele Matthias,[1] Frederick W. Alt,[4] Saadi Khochbin,[2] and Patrick Matthias[1]*

Friedrich Miescher Institute for Biomedical Research, Novartis Research Foundation, P.O. Box 2543, Maulbeerstrasse 66, 4058 Basel, Switzerland[1]; Novartis Institutes for Biomedical Research, Klybeckstrasse, Basel, Switzerland[3]; Howard Hughes Medical Institute, The Children's Hospital, The CBR Institute for Biomedical Research, Harvard Medical School, Boston, Massachusetts 02115[4]; and INSERM U309, Institut Albert Bonniot, Faculté de Médecine, Domaine de la Merci, 38706 La Tronche Cedex, France[2]

Received 27 June 2006/Returned for modification 1 August 2006/Accepted 14 November 2007

Posttranslational modifications play important roles in regulating protein structure and function. Histone deacetylase 6 (HDAC6) is a mostly cytoplasmic class II HDAC, which has a unique structure with two catalytic domains and a domain binding ubiquitin with high affinity. This enzyme was recently identified as a multisubstrate protein deacetylase that can act on acetylated histone tails, α-tubulin and Hsp90. To investigate the in vivo functions of HDAC6 and the relevance of tubulin acetylation/deacetylation, we targeted the *HDAC6* gene by homologous recombination in embryonic stem cells and generated knockout mice. HDAC6-deficient mice are viable and fertile and show hyperacetylated tubulin in most tissues. The highest level of expression of HDAC6 is seen in the testis, yet development and function of this organ are normal in the absence of HDAC6. Likewise, lymphoid development is normal, but the immune response is moderately affected. Furthermore, the lack of HDAC6 results in a small increase in cancellous bone mineral density, indicating that this deacetylase plays a minor role in bone biology. HDAC6-deficient mouse embryonic fibroblasts show apparently normal microtubule organization and stability and also show increased Hsp90 acetylation correlating with impaired Hsp90 function. Collectively, these data demonstrate that mice survive well without HDAC6 and that tubulin hyperacetylation is not detrimental to normal mammalian development.

Protein acetylation/deacetylation is involved in the regulation of protein structure and function, and therefore has potentially important roles in most cellular processes. In particular, the impact of histone N-terminal acetylation on chromatin organization and gene expression has been well documented (15). Acetylation and deacetylation of histone tails or of other proteins are catalyzed by histone acetyltransferases and histone deacetylases (HDACs), respectively. In mammals, there are 18 HDACs identified so far that can be grouped into three classes (reviewed in references 35, 36, and 39). In cells, most, if not all, class I and II HDACs are part of high-molecular-weight complexes that typically contain several HDAC polypeptides and are recruited to DNA via their interactions with sequence-specific or nonspecific DNA-binding proteins.

HDAC 6 (HDAC6) was first identified through its homology to the *Saccharomyces cerevisiae* histone deacetylase HDA1 (9, 34). Like other class II HDACs, HDAC6 is mainly localized in the cytoplasm, but it can also shuttle between the nucleus and cytoplasm (33). This process is regulated by an N-terminally located nuclear export signal and possibly other uncharacterized mechanisms. HDAC6 has not been found in any class I or II HDAC-containing repressor complexes, which suggests it may have a unique regulation and possibly substrates different from those of other HDACs. However, it was shown biochemically and in genome-wide two-hybrid experiments to associate with the class III deacetylase SirT2 (22, 26). Interestingly, HDAC6 contains two hdac catalytic domains in the N-terminal part, and a zinc-UBP domain in the C-terminal part. The zinc-UBP domain in HDAC6 has been shown to interact with high affinity with monoubiquitin, polyubiquitin, and ubiquitinated proteins (2, 13, 28), suggesting that HDAC6 might also be involved in the regulation of protein ubiquitination. In line with this, HDAC6 has been found to facilitate the accumulation of ubiquitinated misfolded proteins into an aggresome (16) and was shown to be important for the induction of heat shock proteins in response to the accumulation of cytotoxic protein aggregates (4). Furthermore, we recently found that HDAC6 is also critical for the formation of stress-induced cytoplasmic granules (19), and the role of HDAC6 as a stress sensor is becoming well established (reviewed in references 3 and 21). We and others independently found that HDAC6 interacts with tubulin and microtubules in the cytoplasm (14, 20, 42). This enzyme is able to deacetylate acetylated lysine 40 in α-tubulin in vitro and in vivo (41, 42) and therefore can

* Corresponding author. Mailing address: Friedrich Miescher Institute for Biomedical Research, Novartis Research Foundation, P.O. Box 2543, Maulbeerstrasse 66, 4058 Basel, Switzerland. Phone: 41-61-697 66 61. Fax: 41-61-697 39 76. E-mail: patrick.matthias@fmi.ch.

† Supplemental material for this article may be found at http://mcb.asm.org/.

‡ Present address: The CBR Institute for Biomedical Research, Harvard Medical School, Boston, MA 02115.

▽ Published ahead of print on 7 January 2008.

modulate the acetylation of microtubules. It has been demonstrated that in human cells HDAC6 can deacetylate heat shock protein 90 (Hsp90) and thereby regulate the chaperone-dependent activation of the glucocorticoid receptor (GR) (1, 17). Very recently, the F-actin-binding protein cortactin was identified as a novel HDAC6 substrate (40). Furthermore, HDAC6 can also deacetylate histone N-terminal tails in vitro. In agreement with this, artificial recruitment of HDAC6 to promoter DNA can repress transcriptional activity, and the deacetylase activity of HDAC6 is necessary for this repression, indicating that it is mediated by HDAC6 directly (Y. Zhang, unpublished results). HDAC6 was also shown to interact with the transcription factor Cbfa1/Runx2 in osteoblasts, resulting in recruitment of HDAC6 into the nucleus and repression of promoters, such as *p21* (37).

In this report, we have generated HDAC6-deficient mice by homologous recombination in embryonic stem (ES) cells. Mice carrying a homozygous deletion of the *HDAC6* gene are viable. We found tubulin acetylation to be significantly increased in most organs of these mice, thus demonstrating that HDAC6 is a bona fide tubulin deacetylase in vivo. While spermatogenesis and development and function of the testis appeared normal, minor phenotypes were identified in the bone and during the immune response. Furthermore, in cells lacking HDAC6, acetylation of tubulin and also Hsp90 was found to be elevated.

Together these results indicate that HDAC6 is dispensable for normal development and that tubulin hyperacetylation, as a result of genetic HDAC6 inactivation or following treatment with HDAC inhibitors, has only minor effects on mice kept under standard laboratory conditions.

MATERIALS AND METHODS

Targeting of the mouse HDAC6 gene in ES cells. The backbone of the targeting vector was subcloned from a bacterial artificial chromosome clone containing the *mHDAC6* gene. The exons encoding the core of the first hdac domain were flanked by a single *loxP* site and a cassette expressing the neomycin resistance gene and thymidine kinase gene flanked by two *loxP* sites (*TK-Neo*^{R} cassette). 129SvOla E14 ES cells were electroporated with the targeting vector, and correctly targeted ES clones were identified by PCR and Southern blot analysis. One targeted ES cell clone (clone 223) was used for transient transfection (electroporation) with the Cre-expressing plasmid pCMV-Cre. Ganciclovir was used to negatively select against clones having retained the *TK-Neo*^{R} cassette and clones containing a knockout (clone 223/124) or a floxed allele (clone 223/126) were identified by PCR, Southern blotting, and DNA sequencing.

Animals. Chimeric mice were crossed to C57BL/6 animals to obtain germ line transmission of the targeted allele. For all analyses, wild-type littermates of the same sex were used as controls. Animal experimentation was carried out according to regulations effective in the canton of Basel-Stadt, Switzerland. The mice were housed in groups of one to six animals at 25°C with a 12-h light-dark cycle (12 h light, 12 h dark). They were fed a standard laboratory diet containing 0.8% phosphorus and 1.1% calcium (NAFAG 890; Kliba, Basel, Switzerland). Food and water was provided ad libitum. Litter size was determined by mating HDAC6-deficient ($n = 20$) or wild-type males ($n = 18$) (3 to 6 months old) together with wild-type females; the number of pups in each cage was counted within a week of birth.

Histological analysis of testis, sperm count, and spermatogenic cell fractionation. For histological analysis of the testis, 3- or 6-month-old mice were used. Paraffin-embedded sections of Bouin-fixed testis were prepared and were stained with hematoxylin and eosin. To determine sperm numbers, cells were collected from cauda epididymides or testis of 12- to 15 week-old mice and allowed to swim up for 15 min in Krebbs Ringer bicarbonate buffer medium containing 1.7 mM $CaCl_2$, pH 7.4 (at 37°C with 5% CO_2), followed by counting under the microscope. The data presented are the averages obtained from three males of each genotype. To examine spermatogenic cell differentiation, cells of all stages were recovered from the testis of adult mice. Cell suspensions enriched in mouse spermatogenic cells at specific differentiation stages (based on cell size and density) were obtained by velocity sedimentation at unit gravity on a bovine serum albumin gradient, according to a method described previously (28).

IHC detection of acetylated histone H4. Ten-micrometer sections were made from paraffin-embedded testis from HDAC6-deficient and wild-type adult male mice. Immunohistochemistry (IHC) was performed as described earlier (11) with an anti-acetyl-histone H4 primary antibody (Upstate) and a biotinylated goat anti-rabbit secondary antibody (Sigma). Testis imprints were made on superfrost slides, and immunofluorescence detection of acetylated H4 was performed as described earlier (11), using the same primary antibody as for IHC, and an Alexa Fluor 488-labeled goat anti-rabbit secondary antibody (Sigma).

Bone analysis by DEXA and pQCT measurements. For dual energy X-ray absorptiometry (DEXA), bone mineral content (mg), area (cm^2), and density (mg/cm^2) of the left tibia was measured using a regular Hologic QDR-1000 instrument adapted for measurements of small animals at 3, 5, and 7 months of age. A collimator with 0.9-cm diameter and ultrahigh-resolution mode (line spacing of 0.0254 cm and resolution of 0.0127 cm) was used. For peripheral quantitative computed tomography (pQCT), cross-sectional bone mineral density, content, and geometry were monitored in the proximal tibia metaphysis 2.5 mm distal from the intercondylar tubercle using an adapted Stratec-Norland XCT-2000 fitted with an Oxford 50-μm X-ray tube and a collimator of 1-mm diameter of animals at 3, 5, and 7 months of age.

FACS, immunization, and enzyme-linked immunosorbent assay (ELISA) analysis. Single-cell suspensions were prepared from the bone marrow, spleen, or thymus of 2- to 3-month-old male mice. Cell staining was done according to standard procedures with lineage- and stage-specific monoclonal antibodies (25). Flow cytometry (FACS) analysis was performed on a FACSCalibur (BD Biosciences, San Jose, CA) by gating on living cells, and 20,000 events were acquired. Samples were analyzed with CellQuest (Becton Dickinson) or Flow-Jo (Tree star) software.

The monoclonal antibodies lineage cocktail 1 (labeled with fluorescein isothiocyanate [FITC]), 7D4 (anti-CD25; biotinylated), 53-6.7 (anti-CD8a labeled with phycoerythrin [PE]), ACK45 (anti-c-kit labeled with PE) were from BD Pharmingen. Monoclonal antibodies 1B4B1 (anti-immunoglobulin M [anti-IgM] labeled with FITC) and GK1.5 (anti-CD4 labeled with FITC) were from Southern Biotech. RA3-6B2 (anti-B220 labeled with allophycocyanin [APC]) and D7 (anti-Ly6A/Sca-1 labeled with APC) were from Biolegend. Avidin-streptavidin labeled with PE Cy5.5 was from Caltag. Mice were immunized with 100 μg of the T-dependent antigen 2,4-dinitrophenyl conjugated to keyhole limpet protein (DNP-KLH). Ten days later, blood samples were collected. Titers for antigen were determined by ELISAs using alkaline phosphatase-labeled anti-IgM or anti-IgG (Southern Biotech) as developing reagents (27).

Establishment of primary MEF and NIH 3T3 cell lines. Mouse embryonic fibroblasts (MEFs) were isolated from mouse embryos at embryonic day 13.5. Sex genotyping was used to select only male embryos. HDAC6-deficient lines were further identified by PCR genotyping and Western blotting. Established MEFs were obtained by following standard NIH 3T3 derivation protocols. SirT2-deficient MEFs have been described previously (32).

Western blotting and immunoprecipitation. Protein extracts were made from either MEFs or mouse tissues and resolved by electrophoresis on 8% or 12% sodium dodecyl sulfate (SDS)-polyacrylamide gels and subsequently blotted to nitrocellulose membranes (Bio-Rad). The antibodies used were mHDAC6 (33), DM1A for α-tubulin or TU6-11 for acetylated tubulin (Sigma), Glu–α-tubulin and Tyr–α-tubulin (Synaptic Systems), and anti-acetyl-histone H4 (Upstate), anti-HDAC-1 and anti-HDAC-2 (gift from Christian Seiser, Vienna Biocenter), and anti-SirT2 (Cell Signaling). To analyze the acetylation of Hsp90, protein extracts were immunoprecipitated with an anti-Hsp90 antibody (Stressgen). Western blotting was performed with anti-acetylated lysine (Cell Signaling) and anti-Hsp90 (Stressgen) antibodies.

Quantification of tubulin acetylation. (i) Immunodepletion. Cells were trypsinized, washed with cold phosphate-buffered saline (PBS), and then lysed for 10 min on ice with a buffer containing 50 mM HEPES (pH 7.5), 300 mM NaCl, 25 mM glycerophosphate, 25 mM NaF, 5 mM EGTA, 1 mM EDTA, 0.5% NP-40, 0.05% sodium deoxycholate, 1 mM phenylmethylsulfonyl fluoride, and the Complete protease inhibitor cocktail (Roche). Lysates were centrifuged 10 min at 4°C. A Polytron was used for homogenization of organs in ice-cold buffer. Protein content of lysates was measured with a BCA protein assay kit (Pierce). Two hundred micrograms of total protein was used for immunoprecipitation with 40 μl of anti-acetyl tubulin and incubated at 4°C overnight. Immunoprecipitates were then recovered by adding 100 μl of protein G-Sepharose 4FF (GE Healthcare) and incubated for 2 h at 4°C. Beads were washed twice with lysis buffer and then resuspended in 200 μl of Laemmli sample buffer. The fractions

corresponding to input, supernatant, and pellet were analyzed by SDS-polyacrylamide gel electrophoresis and immunoblotting.

(ii) Quantification. Serial dilutions of total extracts (cells or tissues) were immunoblotted for acetyl-tubulin or tubulin; each membrane was reprobed for actin (Ab-5; Neomarkers) which was used as an internal loading control. Alexa Fluor 680-labeled goat anti-mouse IgG (Invitrogen) was used as a secondary antibody and detected with an Odyssey system (Li-Cor). Odyssey software was used to quantify the corresponding signals as follows: the signals were measured, and the slopes of the curves obtained with the different dilutions were used in the formula (acetylated tubulin/actin)/(tubulin/actin). Based on the immunoprecipitation results, the ratio obtained in HDAC6 knockout samples was set at 100% tubulin acetylation.

Transient transfections and luciferase reporter assays. MEFs were seeded into six-well plates and allowed to reach ~50% confluence. Cells were cotransfected with 1 μg of MTV-GRE-luciferase reporter and 50 ng of *Renilla* control vector. Dexamethasone was added to the culture medium for the last 4 h of transfection at a concentration of 10^{-7} M. After 48 h of transfection, cell lysates were prepared, and equal protein amounts were analyzed with a Dual-Luciferase reporter assay kit (Promega). Relative luciferase activity was determined by the ratio of firefly luciferase activity to *Renilla* luciferase activity.

Immunofluorescence and microscopy. Exponentially growing cells were plated on BD Falcon eight-chamber slides and incubated overnight. After drug treatment, cells were washed in PHEM buffer [60 mM piperazine-*N*,*N*′-bis(2-ethanesulfonic acid) (PIPES) (pH 6.9), 25 mM HEPES (pH 7.5), 10 mM EGTA (pH 7.5), 4 mM $MgCl_2$ (pH 6.9)] and fixed with methanol at −20°C for 10 min. Slides were rinsed three times with PHEM buffer containing 0.2% Triton X-100, and cells were permeabilized with PBS containing 1% Triton X-100 for 5 min at room temperature. Slides were then incubated in blocking solution (PBS containing 3% bovine serum albumin) for 1 h at room temperature for reducing nonspecific binding of the antibody. Incubation with the primary antibodies was carried out for 3 h at room temperature or overnight at 4°C, and the slides were then washed three times with PHEM buffer containing 0.2% Triton X-100. Alexa Fluor-labeled anti-mouse immunoglobulin antibodies were used as secondary antibodies. After the slides had been washed three times with PHEM buffer containing 0.2% Triton X-100 and once with deionized water, they were observed with a fluorescence microscope (Zeiss Z1). Pictures were deconvolved with the theoretical point spread function calculated within the Huygens Deconvolution software program (Scientific Volume Imaging).

RESULTS

Targeted inactivation of HDAC6 in mice. To directly test the roles of HDAC6 in vivo, we set out to generate knockout mice. For this, exons 8 to 10 encoding the first hdac domain of the HDAC6 gene were flanked by *loxP* sites and a floxed *TK-Neo*^{R} cassette (Fig. 1A). Southern blotting was used to verify the proper targeting in ES cells. As shown in Fig. 1B, two ES clones showed the correctly targeted band at 1.6 kb, while the 4.5-kb wild-type band originates from feeders. The positive clones were used for transient transfection of a Cre recombinase expression vector. After selection against thymidine kinase (*tk*), both floxed and deleted (knockout) clones were identified. As these cells are derived from the ES cell line E14, which has a male genotype, and the HDAC6 gene is on the X chromosome, the deleted cells are deficient for HDAC6 protein and activity (42). Although the absence of HDAC6 resulted in significant tubulin hyperacetylation, these deleted ES cells showed no obvious phenotypes and proliferate normally (42; also data not shown). Floxed and knockout ES cell lines were used for aggregation, and chimeras were obtained, from which mice heterozygous or homozygous for the HDAC6 deletion were derived. The genotype of offspring derived from HDAC6 heterozygous intercrosses was determined by Southern blot analysis and PCR. As the HDAC6 gene is located on the X chromosome, five different genotypes can be obtained with respect to HDAC6 (Fig. 1C).

Both HDAC6 floxed and also knockout animals were obtained at the expected Mendelian ratio, were viable and fertile, and showed no obvious phenotype. Further breeding of HDAC6-deficient mice resulted in approximately Mendelian ratios of progeny with no gender bias. Both HDAC6-deficient male and female mice were indistinguishable from their wild-type and heterozygous littermates by gross observations.

Global tubulin hyperacetylation in HDAC6-deficient mice. To demonstrate the functional ablation of HDAC6, we checked HDAC6 protein expression and measured tubulin acetylation in various tissues from HDAC6-deficient mice. As shown in Fig. 2A, left panel, the HDAC6 protein is predominantly expressed in the testis and is weakly expressed in the brain, kidney, liver, and mammary gland (data not shown). After longer exposure of the film, faint HDAC6 expression can also be detected in the heart and spleen samples. As expected, all HDAC6-specific bands are completely absent from HDAC6-deficient tissues (Fig. 2A, right panel). The remaining signals in the liver and brain samples from HDAC6-deficient mice are nonspecific cross-reacting bands.

Next we examined the level of tubulin acetylation in the absence of HDAC6. As shown in Fig. 2B, tubulin acetylation increased in most tissues examined. Surprisingly, there is no direct correlation between the level of HDAC6 expression in a given tissue and the apparent increase in tubulin acetylation in the corresponding knockout sample: even organs, such as the heart or spleen, which have a very low expression of HDAC6 in wild-type mice, exhibit a strong increase in tubulin acetylation in knockout mice. In contrast, the brains of HDAC6-deficient mice showed no significant increase of tubulin acetylation. However, in the brain, tubulin is already highly acetylated in wild-type animals (Fig. 2B), and therefore, inactivation of the deacetylase in this organ did not have a visible impact on acetylation levels. Experiments were performed to quantify the level of tubulin acetylation in different knockout or wild-type samples (see below and see Fig. 8). As the microtubule network plays important roles in the neuronal system and HDAC6 is significantly expressed in the brain, we examined the central and peripheral nervous systems by histological analysis. However, both the brains and spinal cords in HDAC6-deficient mice were similar to those in wild-type control littermates, and no obvious abnormalities were seen by light microscopic examination (see Fig. S1 in the supplemental material).

Effects of HDAC6 ablation on histone and tubulin acetylation during spermatogenesis. The highest level of HDAC6 expression had been observed in the testis (Fig. 2) (28). This indicates that HDAC6 could play an important role in this organ and could participate in the control of protein acetylation-dependent events taking place during spermatogenesis. Because of this, we first examined testis morphology and functionality. As shown in Fig. 3A, histological examination of sections revealed no difference between wild-type and HDAC6-deficient testes. In addition, sperm were counted after collection from either the testis or epididymis, and similar numbers were obtained from both genotypes (Fig. 3B). Furthermore, knockout and wild-type males were compared in mating experiments with wild-type females; however, the resulting litters showed no significant size differences (Fig. 3C).

We had previously shown that in the mouse, during spermiogenesis the postmeiotic maturation of cells is associated

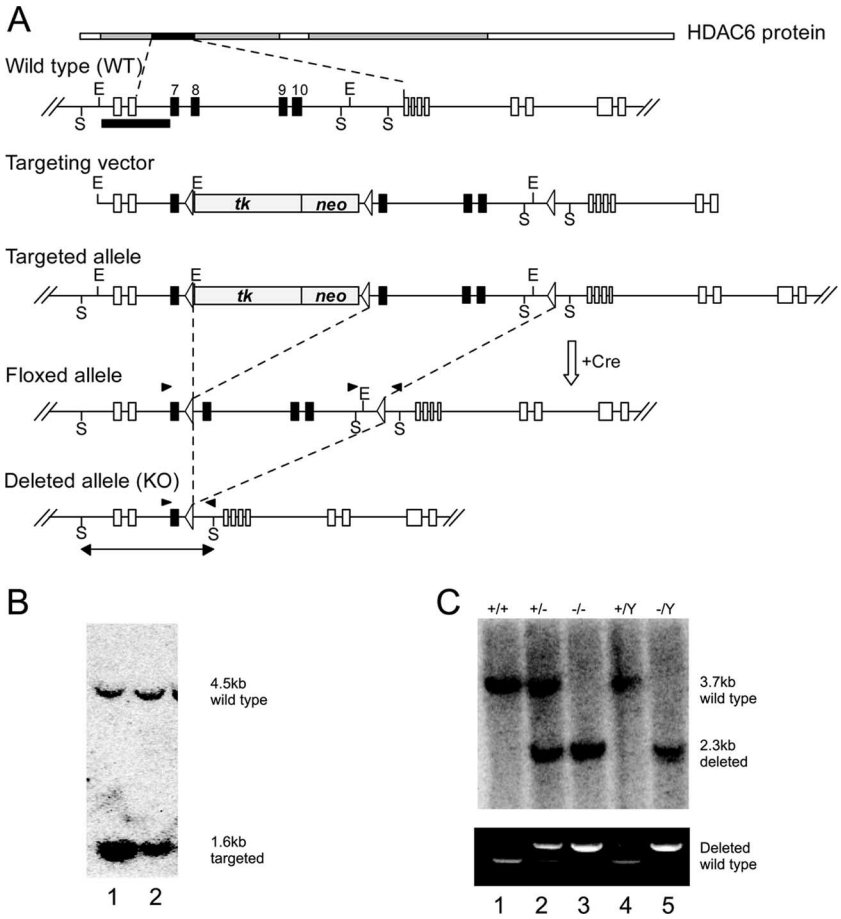

FIG. 1. Generation of HDAC6-deficient mice. (A) Conditional knockout strategy for the targeted disruption of the *HDAC6* gene in the mouse. A targeting vector was constructed by inserting a *loxP* site in intron 10 and a floxed *TK-Neo*^{R} cassette in intron 7. Open arrowheads represent the *loxP* sites. The conditional allele was generated by transiently transfecting targeted ES cells with a Cre expression plasmid to remove the *TK-Neo*^{R} cassette, thus leaving two *loxP* sites flanking exons 8 and 10. The null allele was generated simultaneously by removing all *loxP*-flanked regions. The short black bars indicate the positions of the probe used in Southern hybridizations. Vertical lines indicate restriction sites: E, EcoRI; S, SacI. KO, knockout. (B) Identification of the targeted clones. G418-resistant ES cells were screened for homologous recombination by PCR and Southern hybridization. A 1.6-kb EcoRI fragment for the targeted allele was detected by the probe. The 4.5-kb band corresponds to the wild-type allele originating from the feeder cells. (C) Mouse genotyping by Southern blotting and PCR. (Top) The 3.7-kb SacI fragment comes from the wild-type allele, and the 2.3-kb band is derived from the null allele. Lanes 1 to 5 contain DNAs from wild-type female, heterozygous female, homozygous null female, wild-type male, and null male mice, respectively. (Bottom) The same DNAs were used for PCR genotyping. The top band represents the null allele, and the bottom band comes from the wild-type allele. The primers used for genotyping are depicted by black arrowheads.

with a dramatic increase in the level of histone acetylation (11). We therefore wondered whether the absence of HDAC6 would affect the level or timing of histone acetylation taking place in stage 8 to 10 spermatids. A detailed analysis of the presence of acetylated histone H4 in testis germinal cells from adult HDAC6-deficient mice performed by immunofluorescence and IHC showed that this is however not the case (Fig. 4A). The appearance of a sudden and widespread histone H4 hyperacetylation was observed both in HDAC6-deficient and wild-type stage 8 spermatids. In mice of both genotypes, this acetylation persists in stage 9 spermatids and disappears before stage 11 (Fig. 4A, top panel). Furthermore, immunofluorescence analysis showed that the intranuclear distribution of the genomic regions associated with hyperacetylated histone H4 were also identical in elongating spermatids, irrespective of the presence of HDAC6 (Fig. 4A, bottom panel). We next monitored the acetylation of tubulin and histone H4 in fractionated mouse spermatogenic cells. Figure 4B shows that in wild-type cells, the level of tubulin acetylation is regulated during spermatogenesis: a slight increase in acetylation is observed at the initiation of the elongation process (cells present in the round spermatid fraction [lane 6]), and tubulin becomes strongly acetylated in condensing and elongating spermatids when the flagellum is in the course of formation (condensing and elongating fraction [lane 8]). Strikingly, a very high level of tubulin acetylation can be observed in HDAC6-deficient spermatogenic cells, which is constant in all differentiation stages examined (lanes 1 to 4). In contrast, the level of H4 acetylation is not significantly different in wild-type or HDAC6-deficient spermatids. These data demonstrate that, although HDAC6 normally down-regulates the level of tubulin acetylation in early spermatogenic cells, the deregulation of this process observed in HDAC6-deficient mice does not impair spermatogenesis.

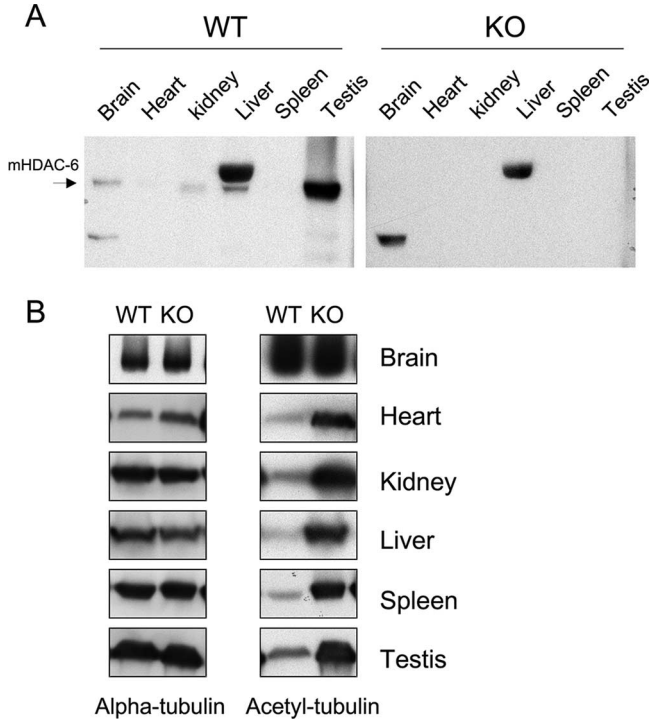

FIG. 2. Inactivation of HDAC6 in vivo leads to tubulin hyperacetylation. (A) Absence of HDAC6 protein in HDAC6-deficient mice. Protein extracts from either HDAC6 wild-type (WT) or deficient (knockout [KO]) male mice were analyzed by Western blotting with an antibody against HDAC6. The mouse HDAC6-specific band is marked by an arrow. The strong band in the liver sample is a cross-reacting protein. (B) Tubulin hyperacetylation in HDAC6-deficient mice. Protein extracts from the indicated organs were immunoblotted for α-tubulin as a loading control and acetylated tubulin to analyze tubulin acetylation.

The lack of HDAC6 has a small effect on bone development. HDAC6 has been shown to interact with the bone-specific transcription factor Runx-2/Cbfa-1 and mediate transcriptional repression of the $p21^{CIP/WAP1}$ promoter in differentiating osteoblasts; this led to the suggestion that this enzyme may play a role in bone development and/or homeostasis (6, 37). Therefore, we examined the skeletal gross anatomy of HDAC6-deficient mice at skeletal maturity by radiography and found no differences (Fig. 5A). As shown in Fig. 5B, the body weight of HDAC6-deficient mice was very slightly elevated at 3 and 5 months of age but was comparable to that of wild-type controls by 7 months of age. We next quantitatively determined several bone parameters by DEXA and pQCT. The tibial bone mineral content (Fig. 5D) was slightly higher at the 3- and 5-month scanning time points, related to the slightly increased bone size, which was reflected in the bone mineral area (Fig. 5C). Overall bone mineral density was slightly increased at 3 months of age but not significantly different at later ages (Fig. 5E). Detailed analysis of the proximal tibia metaphysis indicated again a marginally higher cross-sectional bone mineral density at 3 months of age, while at 5 and 7 months of age, bone mineral density was comparable to that of the wild-type control at this scanning site. The slightly increased bone diameter seen in the periosteal circumference of the proximal metaphysis at the first two scanning time points (Fig. 5G) is consistent with the minimal increase in bone size detected by DEXA (Fig. 5C). The most pronounced effect was on cancellous bone mineral density, which was moderately, yet significantly, higher at all time points (Fig. 5I). This increase was however not substantial enough to result in significantly increased overall density in the metaphyseal cross section (Fig. 5F).

Because HDAC6 can interact with Runx-2/Cbfa-1 (37; also data not shown), we crossed HDAC6-deficient mice with *colI-Cbfa1* transgenic mice overexpressing Cbfa-1 from the collagen type I promoter in bone (8). The compound transgenic mice showed the expected bone phenotype characteristics of the *colI-Cbfa1* mice (low bone mass and multiple bone fractures [8]), which were not affected by the presence or absence of HDAC6 (data not shown).

The absence of HDAC6 does not impair lymphocyte development but moderately impacts the immune response. We also examined whether the absence of HDAC6 has an impact on the development of lymphocytes or on their function. For this, we examined the bone marrow, thymus, and spleen by flow cytometry, using a battery of monoclonal antibodies against cell- and stage-specific surface markers. The results of a representative FACS analysis are presented in Fig. 6A, and quantified data from several mice are shown in Fig. 6B. In the bone marrow, the hematopoietic progenitor cell compartment ($Sca1^+$ Lin^-), representative of cells that are not yet committed to the lymphoid cell lineage, is present at normal numbers. The different stages of early B-cell development (pro-B, $B220^+$ $c\text{-}kit^+$; pre-B, $B220^+$ $CD25^+$; immature, $B220^+$ IgM^+ and mature, $B220^{hi}$ IgM^+) are also all found in similar proportions in the bone marrow. Similarly, early T-cell development in the thymus shows no difference between wild-type and HDAC6-deficient mice: neither the double-negative ($CD4^-$ $CD8^-$) or double-positive ($CD4^+$ $CD8^+$) cells nor the single-positive ($CD4^+$ or $CD8^+$) cells are altered. Furthermore, in the spleen, the proportions of the different mature B-cell populations expressing surface immunoglobulins ($B220^+$ IgM^+ or $B220^+$ IgD^+) or T-cell populations ($CD4^+$ or $CD8^+$) are similar in the two genotypes. We therefore conclude that lymphocyte development proceeds normally in the absence of HDAC6.

We next determined serum immunoglobulin levels in $HDAC6^{-/y}$ mice and control $HDAC6^{+/y}$ littermates, as well as the capacity of these animals to mount an immune response. As shown in Fig. 6C, in unchallenged mice, serum IgM and IgG levels of $HDAC6^{-/y}$ mice were close to the normal values seen in wild-type littermate controls. When mice were immunized with the T-cell-dependent antigen DNP-KLH, a robust response of anti-DNP specific IgGs was observed in wild-type mice, as expected; in HDAC6-deficient mice, however, a ca. fourfold-weaker response was obtained. Thus, HDAC6 appears to have a small impact on the immune response.

HDAC6-deficient MEFs show an increase in tubulin and Hsp90 acetylation. We established MEFs from HDAC6-deficient and control wild-type mice. As shown in Fig. 7A, HDAC6-deficient MEFs completely lacked HDAC6 expression at RNA or protein level and this led to α-tubulin hyperacetylation. In addition, the acetylation of Hsp90 also increased in the HDAC6-deficient MEFs (Fig. 7B and see below), consistent with what was shown recently in human cells by short hairpin RNA-mediated knockdown of HDAC6 (1,

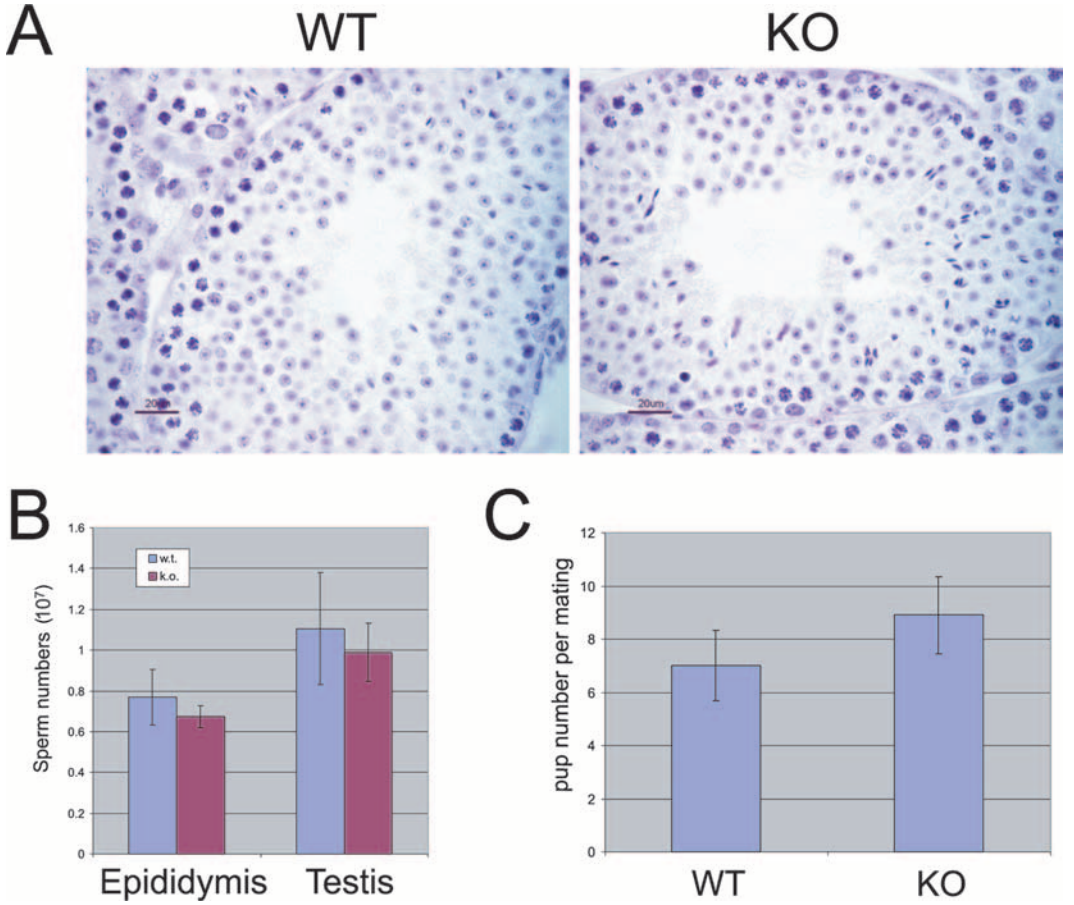

FIG. 3. The absence of HDAC6 does not affect testis architecture, fertility, and sperm count. (A) Testis sections from HDAC6-deficient (knockout [KO]) and wild-type (WT) mice are shown following hematoxylin and eosin staining. (B) Average pup numbers per litter ($n > 15$) were determined from matings between HDAC6-deficient (knockout [k.o.]) or wild-type (w.t.) males and wild-type females. (C) Sperm counts from epididymides or testis.

17). Together, these results suggest that HDAC6 is a deacetylase for tubulin and Hsp90, as well as for cortactin, as recently demonstrated (40). Whether HDAC6 deacetylates other substrates under certain conditions or in specific cells remains to be tested.

To determine accurately the level of tubulin acetylation in wild-type or knockout cells, a specific assay was devised. For this, we first determined conditions under which acetylated tubulin could be quantitatively immunoprecipitated from cell extracts containing depolymerized tubulin (not shown). Following this, the total amount of tubulin (acetylated and nonacetylated) present in the input, supernatant, and pellet fractions was evaluated by Western blotting. It is important to note that in these assays, equivalent relative amounts of the different fractions (input, supernatant, and pellet) were loaded on the gel, thus allowing a direct comparison between the input and supernatant. As presented in Fig. 8A, when acetylated tubulin is completely immunodepleted from wild-type MEF extracts, a large fraction of the total tubulin remains in the supernatant (compare lanes 2 and 3). In contrast, when the same experiment is done with extracts from HDAC6-deficient MEFs, all the tubulin is immunoprecipitated by the anti-acetyltubulin antibody (lanes 5 and 6). This observation therefore indicates that in these cells, essentially all of the tubulin is acetylated. This information was used to determine the relative amount of acetylated tubulin in wild-type cells. For this, serial dilutions of extracts were prepared, and the amount of acetylated or total tubulin was accurately determined by Western blotting (see Materials and Methods). As shown in Fig. 8B, in wild-type MEFs, about 20 to 25% of the tubulin is acetylated. Hence, in MEFs, the knockout of HDAC6 results in a four- to fivefold increase in the level of tubulin acetylation. Using this procedure, we also determined the level of tubulin acetylation in several mouse organs. In each case tested, we found that quantitative immunoprecipitation of acetylated α-tubulin led to complete depletion of the tubulin from the HDAC6 knockout samples (data not shown). In contrast, the wild-type samples showed various levels of acetylated tubulin, from only ca. 2 to 3% in testis to about 100% in brain, in good agreement with the qualitative picture presented in Fig. 2B and 4B. Furthermore, the spleen sample had about 25% of acetylated tubulin, similar to what is seen in MEFs. Thus, wild-type cells or organs have widely different levels of acetylated α-tubulin.

HDAC6 is the major tubulin deacetylase. It has been previously demonstrated that SirT2 interacts with HDAC6 and is a NAD^+-dependent tubulin deacetylase (22). We have therefore

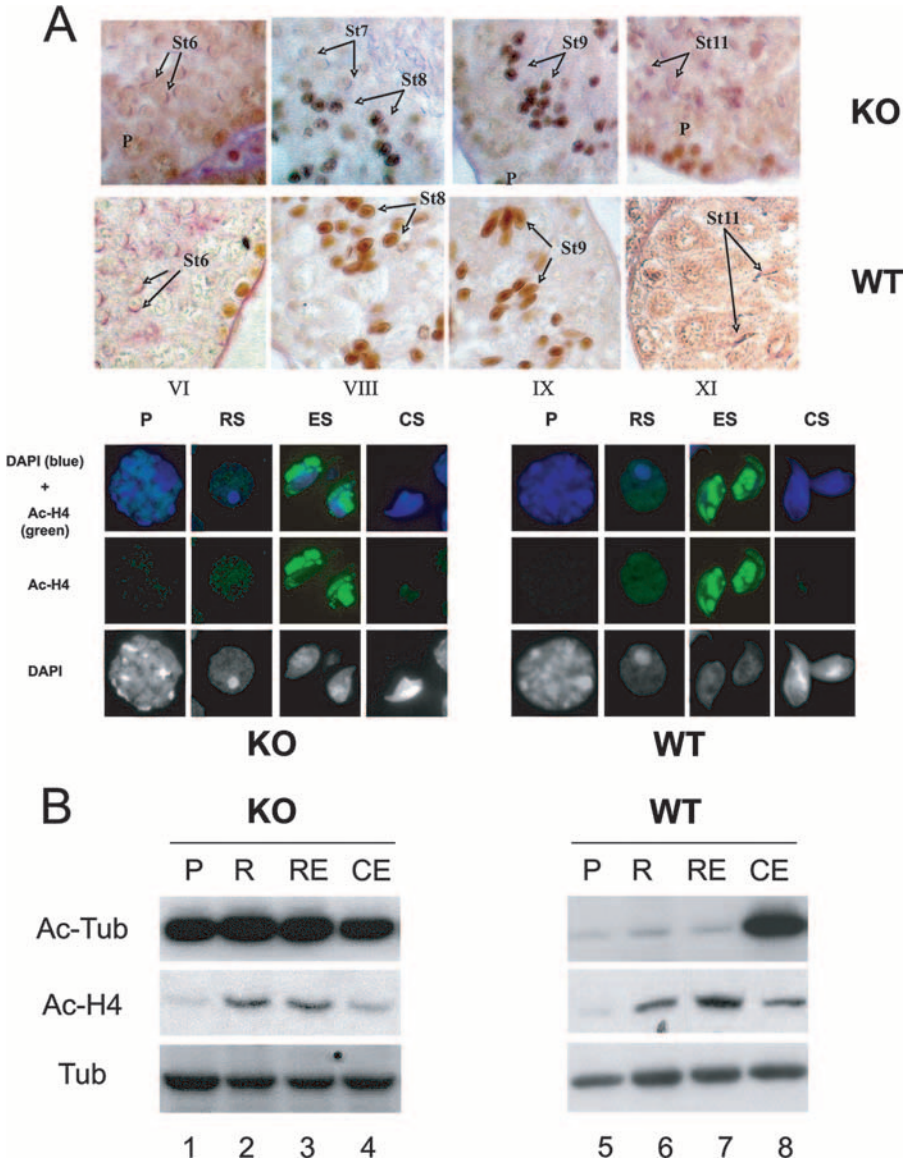

FIG. 4. Inactivation of HDAC6 induces tubulin hyperacetylation during spermatogenesis but does not alter histone H4 acetylation. (A) The patterns of histone H4 acetylation during spermatogenesis are similar in HDAC6-deficient (knockout [KO]) and wild-type (WT) mice. (Top) Detection of acetylated H4 by immunohistochemistry on paraffin-embedded testis sections. Pachytene cells (P) and spermatid stages 6 (St6) to 11 (St11) are indicated. (Bottom) Detection of acetylated H4 by immunofluorescence on paraformaldehyde-fixed germinal cells. Abbreviations: P, pachytene cells; RS, round spermatids; ES, elongating spermatids; CS, condensing spermatids; DAPI, 4′,6′-diamidino-2-phenylindole; Ac-H4, acetylated histone H4. (B) Tubulin acetylation in HDAC6-deficient and wild-type spermatogenic cells. Spermatogenic cells were dissociated and fractionated, and the corresponding extracts were analyzed by immunoblotting to monitor tubulin acetylation (Ac-Tub), histone H4 acetylation (Ac-H4), and α-tubulin (Tub). The fractions analyzed were enriched in the following types of spermatogenic cells: pachytene spermatocytes (P), round spermatids (R), round and elongating spermatids (RE), and elongating and condensing spermatids (CE).

tested whether SirT2—or another HDAC—could contribute to tubulin deacetylation in these cells. For this, HDAC6-deficient cells were treated with nicotinamide, a SirT2 inhibitor, or trichostatin A (TSA), a general class I and class II HDAC inhibitor. As shown in Fig. 9A, TSA treatment increased tubulin acetylation levels in wild-type MEFs to the same extent as that observed for HDAC6-deficient MEFs. In addition, TSA treatment did not further increase tubulin acetylation in HDAC6-deficient MEFs (compare lanes 4 and 5). Furthermore, treatment by nicotinamide did not affect tubulin acetylation in either wild-type or HDAC6-deficient MEFs. To definitively establish whether SirT2 contributes to tubulin acetylation in fibroblasts, we next made use of SirT2 knockout cells and the corresponding control MEFs and performed immunoprecipitation and extract serial dilution experiments as described above (Fig. 8). As shown in Fig. 9B, quantitative immunoprecipitation of acetylated tubulin from wild-type MEFs led to only partial depletion of tubulin, similar to what was shown in Fig. 8A. Strikingly however, the same result was obtained in SirT2 knockout MEFs, which exhibited the same

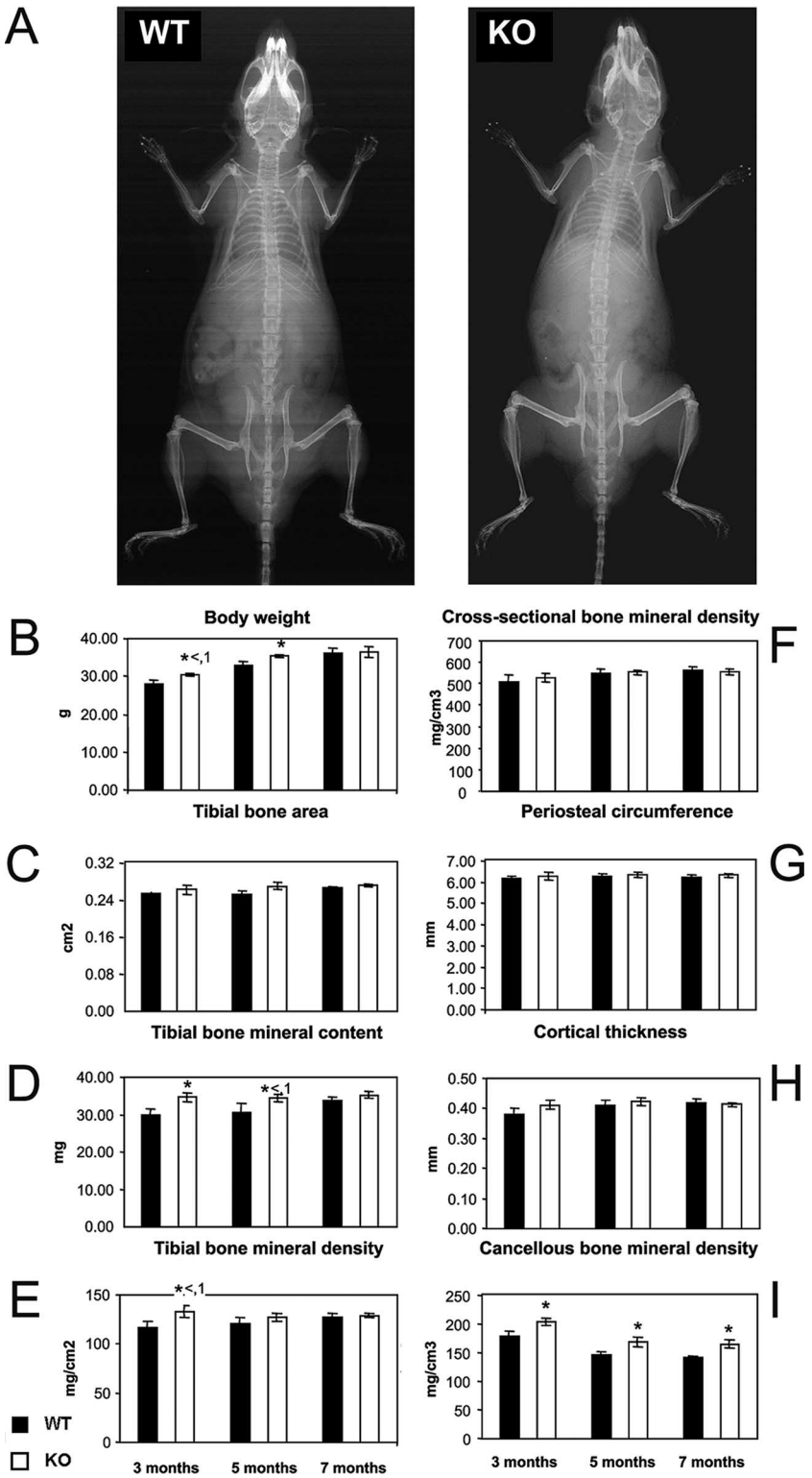

FIG. 5. Analysis of the skeletal anatomy of HDAC6-deficient mice. Bone mass analyses of HDAC6-deficient mice were performed. (A) Whole-body radiographs of 7-month-old male mice. One wild-type (WT) mouse and one HDAC6-deficient (knockout [KO]) mouse are depicted. (B) Body weight at 3, 5, and 7 months of age. (C to E) DEXA analysis of tibial bone area and bone mineral content and density. (F to I) pQCT analysis of a cross section through the proximal tibia metaphysis at 3, 5, and 7 months of age: cross-sectional bone mineral density, periosteal circumference, cortical thickness, and cancellous bone mineral density. All results are presented as means ± standard errors of the means (error bars). Values for the HDAC6-deficient (knockout [KO]) mice that were significantly different ($P > 0.05$) from the value for wild-type mice are indicated by an asterisk.

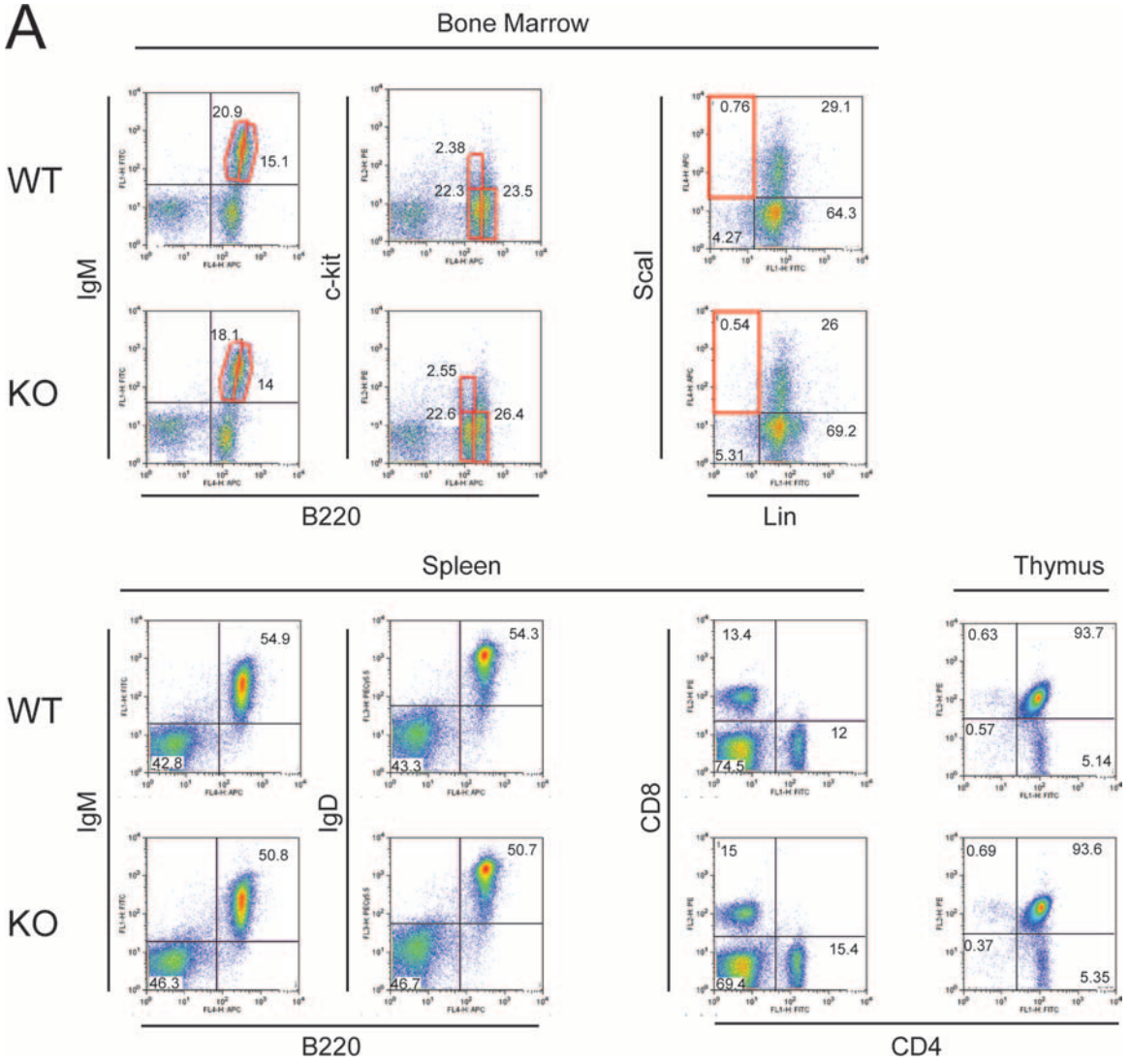

FIG. 6. Analysis of lymphocyte development and immune response in HDAC6-deficient mice. (A) FACS analysis of 10-week-old wild-type (WT) or HDAC knockout (KO) mice. Bone marrow cells, thymocytes, or splenocytes were analyzed by flow cytometry after staining with FITC-, PE-, PE Cy5.5-, and APC-conjugated antibodies. The dot plots show data from one representative animal of each genotype; the percentage of cells in the respective quadrants are indicated. (B) The proportions of the different cell populations analyzed are presented as histograms showing the means ± standard deviations (error bars) of data from five mice of each genotype. The proportions of double-negative (DN), double-positive (DP), $CD4^+$, and $CD8^+$ cells from the thymus are shown. (C) Moderately impaired immune response in the absence of HDAC6. Wild-type and HDAC6-deficient mice were immunized with DNP-KLH, and 10 days later, serum immunoglobulin levels were measured by ELISAs ($n = 4$). Each symbol shows the value for one mouse, and the bar shows the mean for the four mice in each group.

amount of acetylated tubulin as the control cells. Subsequent quantifications showed that in wild-type and SirT2-deficient cells, the level of acetylated tubulin is around 20 to 25%. Thus, genetic inactivation of SirT2 fails to alter the level of tubulin acetylation in MEFs. These findings indicate that, in MEFs at least, HDAC6 is the only tubulin deacetylase with detectable in vivo activity toward tubulin.

Previous studies have suggested that HDAC6-mediated tubulin deacetylation reduces microtubule stability (20) and promotes cell motility (14). Yet, other recent studies failed to see increased stability of microtubules following inhibition of HDAC6 (10, 23). We have therefore reexamined the roles of HDAC6, and deacetylases in general, on microtubule stability and used for this a previously published experimental scheme (20) with HDAC6 knockout MEFs, wild-type MEFs, and knockout MEFs reexpressing HDAC6. The cells were treated with different combinations with HDAC inhibitors and/or a microtubule-destabilizing agent, and the microtubule network was examined by microscopy at different time points; furthermore, tubulin acetylation was also examined biochemically. However, in these experiments, which are presented in Fig. S2 in the supplemental material, we did not observe a clear effect of HDAC6 on the stability of the microtubule network.

HDAC6-deficient MEFs are defective in GR translocation and GR-mediated transcription activation. It has been recently shown that in human cells HDAC6 can deacetylate the

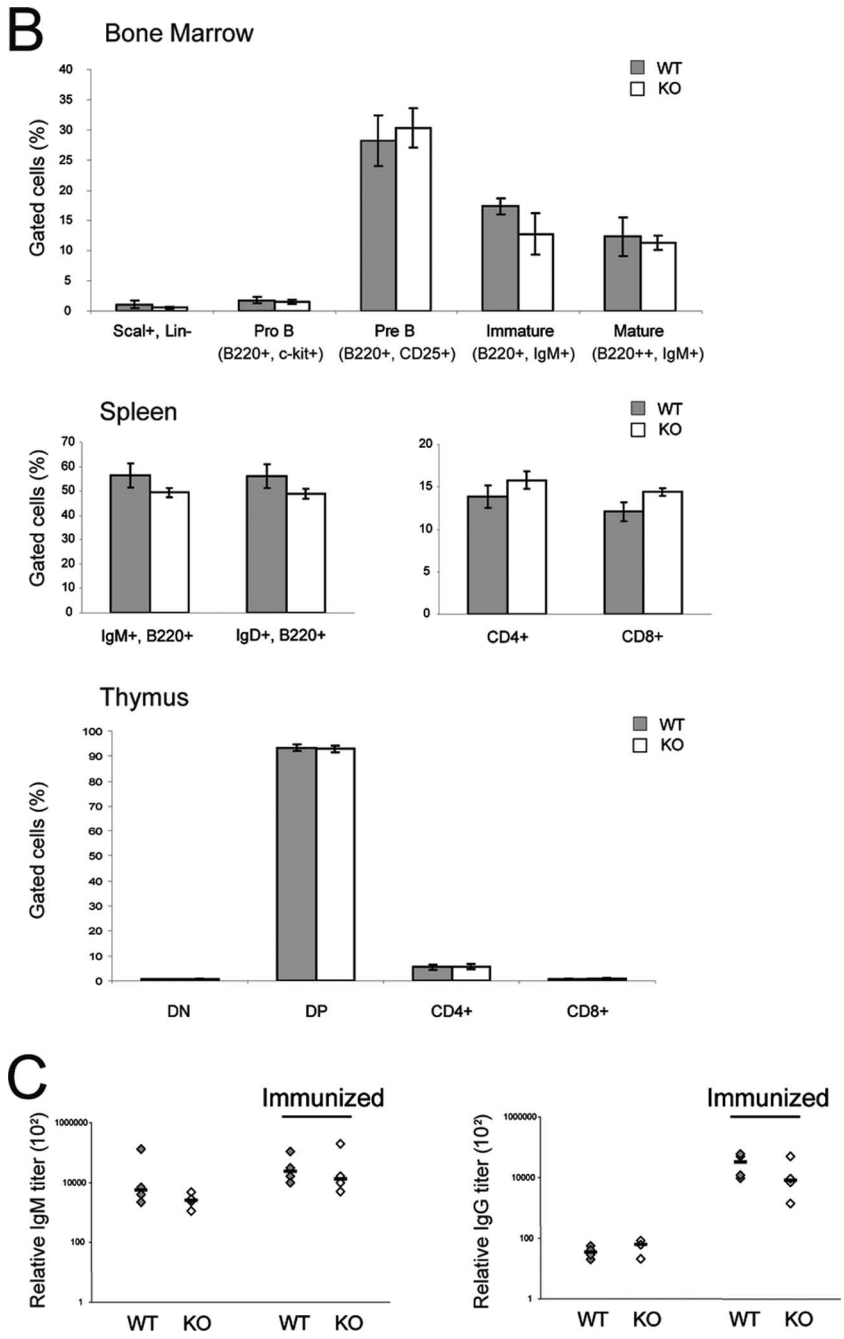

FIG. 6—*Continued*.

chaperone Hsp90 and that small interfering RNA-mediated knockdown of HDAC6 impairs activation of the glucocorticoid receptor or other client proteins (1, 17). In the absence of hormone, the GR is kept in a cytoplasmic complex with the chaperone Hsp90, whose function is critical to promote maturation of the GR into a form that is competent for ligand binding. We have demonstrated here that Hsp90 is hyperacetylated in MEFs lacking HDAC6 (Fig. 7B) and have set out to test whether this has functional consequences for GR activation. For this, we used the three MEF lines shown in Fig. 8, as well as knockout MEFs reexpressing either a catalytically inactive HDAC6, or a ubiquitin-binding defective version of HDAC6. A GR-dependent luciferase reporter was transiently transfected into the different cell lines, together with a reference plasmid. As shown in Fig. 10A, upon hormone treatment, wild-type cells showed a 10-fold activation of the reporter, while cells lacking HDAC6 exhibited only ca. 3.5-fold activation; furthermore, cells reexpressing wild-type HDAC6 showed nearly the same activation as wild-type cells did. Remarkably, cells expressing a deacetylase-defective or a non-ubiquitin-binding HDAC6 were impaired in activation at least as much as the knockout cells were. These results do not reflect altered

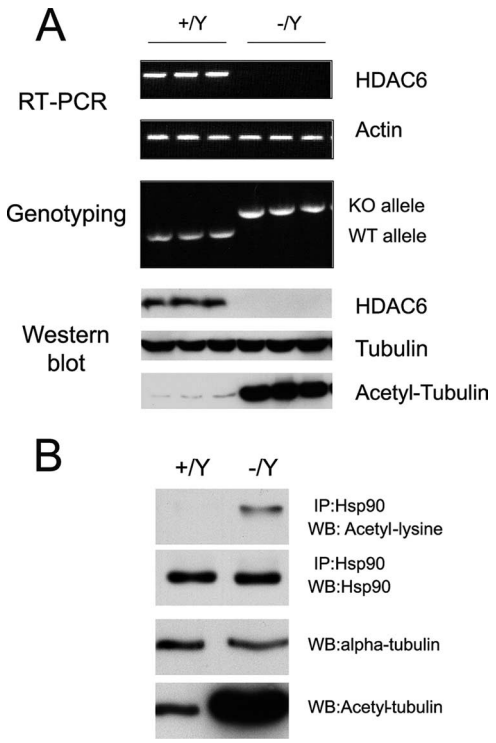

FIG. 7. HDAC6-deficient MEFs show increased tubulin and Hsp90 acetylation. (A) MEFs were derived from HDAC6-deficient (−/Y) and wild-type (+/Y) male embryos. Three independent lines are presented for each genotype. Reverse transcription-PCR (RT-PCR) was performed for mouse HDAC6 using 3′ primers on exon 8 which is deleted in the null allele. Actin was used as a loading control. PCR genotyping was performed to confirm the genotypes (knockout [KO] and wild-type [WT]) alleles. Protein extracts from individual cell clones were used for Western blotting with antibodies against mouse HDAC6, α-tubulin, and acetyl-tubulin. (B) Increased tubulin and Hsp90 acetylation in HDAC6-deficient MEFs. Hsp90 was immunoprecipitated (IP), and acetylation was examined with an antibody recognizing acetyl-lysine. WB, Western blotting.

GR levels in the different cell lines, and the Western blot presented in Fig. 10B demonstrates that GR protein expression is not modulated by HDAC6. We therefore examined hormone-induced nuclear translocation of the GR; as shown in Fig. 10C, hormone addition leads to nuclear translocation of the GR in wild-type cells, but not in HDAC6-deficient cells. Together, these data indicate that Hsp90 deacetylation by HDAC6 is necessary for the activation of the GR and possibly other proteins.

DISCUSSION

Here, we generated and analyzed mice lacking the deacetylase HDAC6. In these mice, greatly elevated tubulin acetylation was observed in most tissues. Therefore, this represents the first in vivo mammalian model for tubulin hyperacetylation. Our results demonstrate that HDAC6 is dispensable and that the level of tubulin acetylation is not critical for embryonic development and adult homeostasis.

Because HDAC6 is expressed the most in the testis, we first examined the development and function of this organ. However, histological analysis of the testis revealed no abnormality in HDAC6 knockout mice; furthermore, the testis is also fully functional, as evidenced from the normal fertility of HDAC6-deficient males (Fig. 3). Isolation and analysis of spermatogenic cells of different stages revealed that the absence of HDAC6 led to a dramatic increase in tubulin acetylation already at an early developmental stage (pachytene spermatids [Fig. 4B]), and this showed no impact on the developmentally regulated acetylation of histone H4. Thus, by several criteria, we found that the lack of HDAC6—as well as the resulting tubulin hyperacetylation—does not impair function of the testis.

We next analyzed bone development, as previous studies had indicated a possible function for HDAC6 in this organ. In particular, it had been shown that the bone-specific transcription factor Runx2/Cbfa1 interacts with HDAC6 and recruits it into the nuclei of osteoblasts, thereby repressing transcription of the *p21* gene (37). This suggests that HDAC6 may also be recruited to other targets of Runx2/CBFA-1 in differentiating osteoblasts to regulate tissue-specific gene expression and that it can contribute to bone development. We found the gross skeletal anatomy to be similar in HDAC6-deficient and wild-type mice. Yet, the metabolically most active bone compartment, the cancellous bone of the tibia metaphysis, displays slightly increased density at both later scanning time points (Fig. 5), thus identifying a minor role for HDAC6 in bone biology. Further studies will be required to elucidate the exact mechanism underlying this phenotype and whether it reflects function of HDAC6 in the nucleus (37) or in the cytoplasm (6). Nevertheless, the possibility that HDAC6 may control gene transcription by deacetylating histones in some select cases will need further detailed study. In agreement with this possibility, we observed that artificial recruitment of HDAC6 to promoter DNA leads to transcriptional repression, which is dependent on the integrity of the hdac domains (Y. Zhang, unpublished data). This is also in good agreement with our previous findings, showing that purified HDAC6 is able to efficiently deacetylate histones in vitro (41).

We also examined lymphoid cell development and function in the absence of HDAC6. We found that in the bone marrow of mice lacking HDAC6, cells representing all the different stages of B-cell differentiation were present at normal numbers; likewise, thymocytes in the thymus were not affected. Furthermore, mature B and T cells were also present in normal numbers in the spleen (Fig. 6B). Therefore, lymphoid development is normal in the absence of HDAC6. However, when mice were immunized with the T-cell-dependent antigen DNP-KLH, a small but significant reduction in the production of antigen-specific IgGs was observed (Fig. 6C). Hence, HDAC6 appears to play a role in the immune response; future work will dissect the molecular basis of this phenotype and define its cellular origin. It is interesting to note that recent experiments with human T cells have identified a role for HDAC6 in the formation of the immune synapse (29). Also, it was shown that lymphocyte chemotaxis is influenced by HDAC6, albeit apparently independently of its deacetylase activity (5). In addition, infection of $CD4^+$ T cells by human immunodeficiency virus was found to be enhanced upon HDAC6 knockdown (31). Thus, HDAC6 appears to impinge on the function of the immune system at different levels.

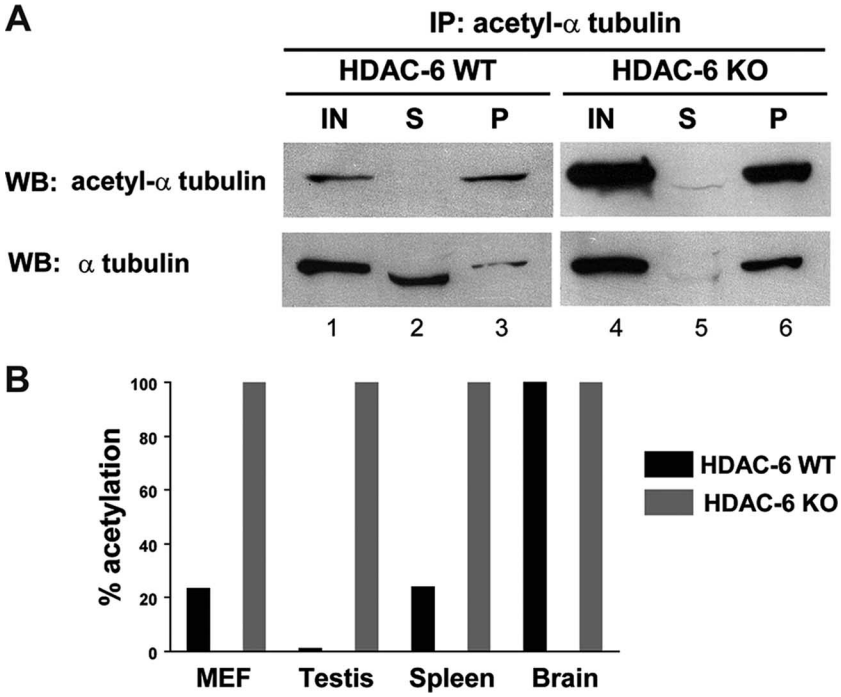

FIG. 8. α-Tubulin is fully acetylated in primary HDAC6 knockout MEFs. (A) Immunodepletion of acetyl-tubulin was performed with extracts from wild-type (WT) and HDAC6 knockout (KO) primary MEFs. Input (IN) (lanes 1 and 4), supernatant (S) (lanes 2 and 5), and pellet (P) (lanes 3 and 6) fractions were analyzed by SDS-polyacrylamide gel electrophoresis followed by immunoblotting (Western blotting [WB]) with an antibody against acetylated α-tubulin or against α-tubulin; in each case, an amount equivalent to 4% of the initial sample was loaded. IP, immunoprecipitation. (B) Percentage of tubulin acetylation in MEFs and mouse organs. Quantification of tubulin acetylation level in wild-type and HDAC6 knockout primary MEFs, testis, spleen, and brain extracts. Immunoblot quantification of serial extract dilutions was done as described in Materials and Methods; the level of acetylation in the knockout sample was set at 100%. Data of one representative experiment are presented ($n = 2$ or 3).

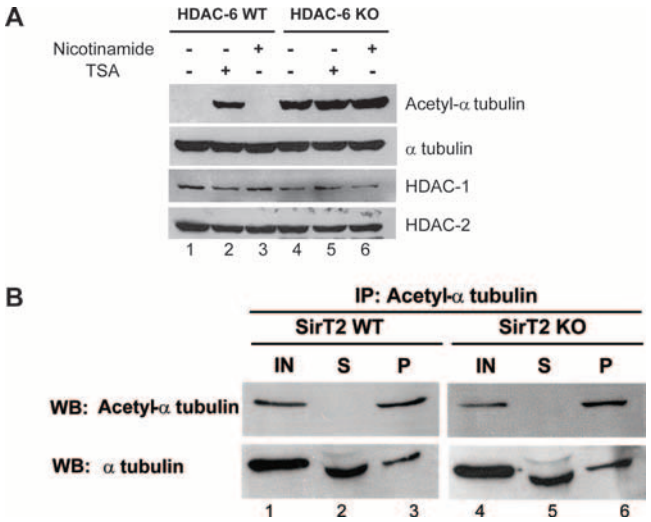

FIG. 9. HDAC6 is the only active tubulin deacetylase in MEFs. (A) Wild-type (WT) and HDAC6-deficient (knockout [KO]) MEFs were treated (+) with either 5 mM nicotinamide or 1.5 μM TSA as indicated. Whole-cell extracts were then analyzed by Western blotting with specific antibodies against acetylated α-tubulin, α-tubulin, HDAC1, or HDAC2. (B) Immunodepletion and immunoblotting experiments were done as described in the legend to Fig. 8A, with wild-type or SirT2 knockout MEF extracts.

We also analyzed the function of HDAC6 in primary or established MEFs. In these cells, as in the mouse organs, acetylation of tubulin and also Hsp90 was increased (Fig. 7 and 8). We quantified the level of tubulin acetylation in fibroblasts and several mouse organs and found it to be spread over a wide range, from close to 100% in brain extracts to as little as a few percent in testis samples (Fig. 8). Furthermore, in every case, the HDAC6 knockout sample showed essentially complete acetylation of tubulin. This indicates that cells are remarkably tolerant to very large changes in the degree of tubulin acetylation. Moreover, we found that in MEFs at least HDAC6 contributes all the tubulin deacetylase activity. Treatment with the SirT2 inhibitor nicotinamide did not further increase tubulin acetylation (Fig. 9), and in agreement with this, MEFs that are deficient in SirT2 also showed no increase in tubulin acetylation. In this context, it should be mentioned that recently SirT2 was shown to localize, during mitosis, to chromatin and to act as a deacetylase for histone H4 acetylated on lysine 16 (H4K16Ac) (32).

Tubulin proteins, the building blocks of microtubules, are subject to several types of evolutionarily conserved posttranslational modifications, including detyrosination, acetylation, generation of Δ2-tubulin, phosphorylation, polyglutamylation, and polyglycylation. Most of these modifications are reversible, and all, except acetylation, occur at the highly variable carboxyl termini of tubulin α and β subunits. Acetylation takes place on lysine 40 of α-tubulin, is mostly associated with stable micro-

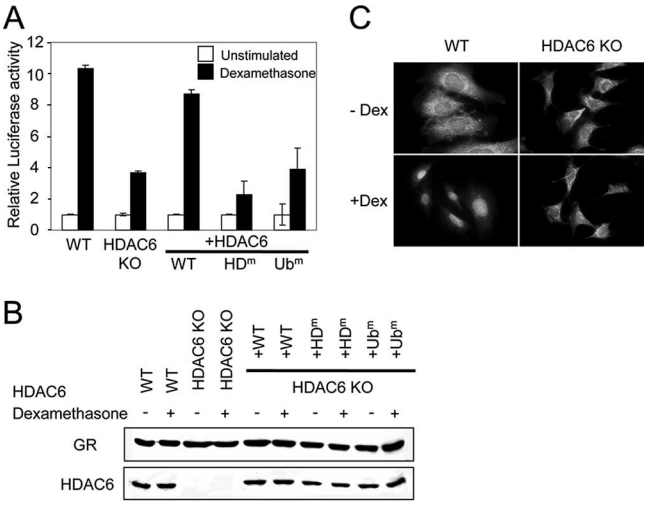

FIG. 10. HDAC6 is required for GR translocation and transcriptional activity. (A) Wild-type (WT) or HDAC6-deficient (knockout [KO]) MEFs or rescuants thereof were transiently cotransfected with an MTV-GRE-firefly luciferase reporter and a *Renilla* luciferase vector as a control. Dual luciferase activity was measured after treatment with dexamethasone, and the ratio of firefly luciferase activity to *Renilla* luciferase activity was used as relative luciferase activity. The rescuant cells express WT HDAC6, a catalytically inactive mutant HDAC6 (HD^m), or a non-ubiquitin-binding mutant of HDAC6 (Ub^m), as indicated. The data are the means of three independent experiments done in triplicate; $P < 0.005$ (WT versus KO). (B) The protein levels of GR and HDAC6 in the different cell lines were determined by immunoblotting with anti-GR and anti-HDAC6 antibodies. The cells were treated with dexamethasone (+) or not treated with dexamethasone (−). (C) Impaired GR translocation in the absence of HDAC6. Wild-type and HDAC6-deficient MEFs were cultured in hormone-free medium for 24 h and then stimulated with dexamethasone (+Dex) for 30 min. The localization of GR was determined by immunostaining with an anti-GR antibody.

tubular structures, such as axonemes, and occurs after microtubule assembly (reviewed in reference 38). The in vivo role of acetylated microtubules in cells and whole animals remains an important unanswered question, although several approaches have already been tried in some eukaryotic organisms and mammalian cell lines. For example, overexpression of a non-acetylatable α-tubulin variant in *Chlamydomonas reinhardtii* (18) or complete elimination of tubulin acetylation by site-directed mutagenesis of the usually acetylated lysine residue to arginine in *Tetrahymena thermophila* (7) had no observable phenotype. Also, disruption of the *HDAC6* gene in mouse embryonic stem cells, which led to highly increased tubulin acetylation levels, did not significantly affect cell proliferation or differentiation of these cells (42). It has been argued that tubulin acetylation is just downstream of microtubule stabilization. Various experiments have shown that tubulin becomes acetylated after microtubules are stabilized. For example, it was recently shown that integrin regulates the stability of microtubules via focal adhesion kinase (FAK) and Rho signals (24). The integrin-FAK signaling pathway may facilitate RhomDia signaling through GM1, or through a specialized membrane domain containing GM1, to stabilize microtubules in the leading edge of migrating cells, and is thereby involved in the regulation of cell migration and motility. A role for tubulin acetylation in cell motility has also been proposed on the basis that HDAC6 overexpression increased the chemotactic movement of NIH 3T3 cells (14), whereas chemical inhibition of HDAC6 impaired cell migration, although it did not change microtubules stability (10). Very recent experiments showed that inhibition of HDAC6 catalytic activity increased the adhesion area of the cell, thus reducing cell migration (30). We also tested, similarly to Matsumaya et al. (20), how HDAC activity influences the resistance of the microtubule network to destabilization by demecolcin. However, in our experiments we could not observe an obvious effect, whether HDAC6 activity was inhibited chemically or genetically and using different experimental setups. In the literature, the relationship between tubulin acetylation and the stability of microtubules has not been seen by all investigators, and this may reflect subtle experimental differences. For example, Palazzo et al. (23) also did not observe that acetylation of the microtubule network led to increased stability. In addition, detyrosination, a tubulin modification which is an established marker of increased microtubule stability, was not found to be elevated in HDAC6-deficient cells (41). Collectively, these data suggest that in vivo tubulin acetylation is not a direct cause for microtubule stabilization but rather could be one of the consequences of increased microtubule stability. The fact that different groups have reported conflicting results on the importance of tubulin acetylation for microtubule stability suggests that this process is still not entirely understood and is difficult to fully control experimentally. The availability of the HDAC6 knockout mice described here and also of overexpression mouse models (our unpublished data) will be instrumental to better understand the role of tubulin acetylation in vivo.

Similar to what had been seen in human cells following HDAC6 knockdown, we also found that Hsp90 is hyperacetylated in MEFs lacking HDAC6. This results in impaired activation of the GR, reflected in defective nuclear translocation of the receptor upon hormone treatment and reduced activation of a GR-dependent reporter gene (Fig. 10), similar to what has been observed in human cells (17). It will be interesting to examine whether other Hsp90-mediated processes are altered in the absence of HDAC6.

HDAC inhibitors appear very promising for cancer therapy, and their mechanism of action is usually considered to be at the epigenetic level, through an increase in histone acetylation; however, most of the inhibitors used so far do not discriminate between classic HDACs and HDAC6. Therefore, they also lead to an increase in acetylation of tubulin, Hsp90, and possible other substrates, and this will have to be considered for clinical applications. The genetic ablation of HDAC6 presented here suggests that pharmacological inhibition of this enzyme may have only a few side effects, at least in a non-pathological setting. In fact, HDAC6 inhibition has recently been considered as a potential way to induce antitumor activity in multiple myeloma cells (12). Nevertheless, the precise in vivo contributions of the different HDACs remain to be better defined in normal and pathological situations.

ACKNOWLEDGMENTS

We thank Patrick Kopp and Jean-François Spetz for excellent assistance with ES cell work and generation of knockout mice, Sandro Rusconi (University of Fribourg) for providing GR reporter plasmids, Christian Seiser (Medical University Vienna) for antibodies against HDAC1 and

HDAC2, and members of the Matthias lab for useful discussions. We also thank Tom McRae (Dalhousie University, Halifax, Nova Scotia, Canada) for generously and rapidly sharing antibodies.

We thank the Novartis Research Foundation for financial support. S. Khochbin's laboratory was supported by the EpiMed and EpiPro (CLARA/INCa) as well as ARECA (ARC) programs. F.W. Alt is an investigator of the Howard Hughes Medical Institute. This work was supported by an Ellison Medical Foundation Senior Scholar Award to F.W.A.

REFERENCES

1. **Bali, P., M. Pranpat, J. Bradner, M. Balasis, W. Fiskus, F. Guo, K. Rocha, S. Kumaraswamy, S. Boyapalle, P. Atadja, E. Seto, and K. Bhalla.** 2005. Inhibition of histone deacetylase 6 acetylates and disrupts the chaperone function of heat shock protein 90: a novel basis for antileukemia activity of histone deacetylase inhibitors. J. Biol. Chem. **280:**26729–26734.
2. **Boyault, C., B. Gilquin, Y. Zhang, V. Rybin, E. Garman, W. Meyer-Klaucke, P. Matthias, C. W. Muller, and S. Khochbin.** 2006. HDAC6-p97/VCP controlled polyubiquitin chain turnover. EMBO J. **25:**3357–3366.
3. **Boyault, C., K. Sadoul, M. Pabion, and S. Khochbin.** 2007. HDAC6, at the crossroads between cytoskeleton and cell signaling by acetylation and ubiquitination. Oncogene **26:**5468–5476.
4. **Boyault, C., Y. Zhang, S. Fritah, C. Caron, B. Gilquin, S. H. Kwon, C. Garrido, T. P. Yao, C. Vourc'h, P. Matthias, and S. Khochbin.** 2007. HDAC6 controls major cell response pathways to cytotoxic accumulation of protein aggregates. Genes Dev. **21:**2172–2181.
5. **Cabrero, J. R., J. M. Serrador, O. Barreiro, M. Mittelbrunn, S. Naranjo-Suarez, N. Martin-Cofreces, M. Vicente-Manzanares, R. Mazitschek, J. E. Bradner, J. Avila, A. Valenzuela-Fernandez, and F. Sanchez-Madrid.** 2006. Lymphocyte chemotaxis is regulated by histone deacetylase 6, independently of its deacetylase activity. Mol. Biol. Cell **17:**3435–3445.
6. **Destaing, O., F. Saltel, B. Gilquin, A. Chabadel, S. Khochbin, S. Ory, and P. Jurdic.** 2005. A novel Rho-mDia2-HDAC6 pathway controls podosome patterning through microtubule acetylation in osteoclasts. J. Cell Sci. **118:**2901–2911.
7. **Gaertig, J., M. A. Cruz, J. Bowen, L. Gu, D. G. Pennock, and M. A. Gorovsky.** 1995. Acetylation of lysine 40 in alpha-tubulin is not essential in *Tetrahymena thermophila*. J. Cell Biol. **129:**1301–1310.
8. **Geoffroy, V., M. Kneissel, B. Fournier, A. Boyde, and P. Matthias.** 2002. High bone resorption in adult aging transgenic mice overexpressing Cbfa1/Runx2 in cells of the osteoblastic lineage. Mol. Cell. Biol. **22:**6222–6233.
9. **Grozinger, C. M., C. A. Hassig, and S. L. Schreiber.** 1999. Three proteins define a class of human histone deacetylases related to yeast Hda1p. Proc. Natl. Acad. Sci. USA **96:**4868–4873.
10. **Haggarty, S. J., K. M. Koeller, J. C. Wong, C. M. Grozinger, and S. L. Schreiber.** 2003. Domain-selective small-molecule inhibitor of histone deacetylase 6 (HDAC6)-mediated tubulin deacetylation. Proc. Natl. Acad. Sci. USA **100:**4389–4394.
11. **Hazzouri, M., C. Pivot-Pajot, A. K. Faure, Y. Usson, R. Pelletier, B. Sele, S. Khochbin, and S. Rousseaux.** 2000. Regulated hyperacetylation of core histones during mouse spermatogenesis: involvement of histone deacetylases. Eur. J. Cell Biol. **79:**950–960.
12. **Hideshima, T., J. E. Bradner, J. Wong, D. Chauhan, P. Richardson, S. L. Schreiber, and K. C. Anderson.** 2005. Small-molecule inhibition of proteasome and aggresome function induces synergistic antitumor activity in multiple myeloma. Proc. Natl. Acad. Sci. USA **102:**8567–8572.
13. **Hook, S. S., A. Orian, S. M. Cowley, and R. N. Eisenman.** 2002. Histone deacetylase 6 binds polyubiquitin through its zinc finger (PAZ domain) and copurifies with deubiquitinating enzymes. Proc. Natl. Acad. Sci. USA **99:**13425–13430.
14. **Hubbert, C., A. Guardiola, R. Shao, Y. Kawaguchi, A. Ito, A. Nixon, M. Yoshida, X. F. Wang, and T. P. Yao.** 2002. HDAC6 is a microtubule-associated deacetylase. Nature **417:**455–458.
15. **Jenuwein, T., and C. D. Allis.** 2001. Translating the histone code. Science **293:**1074–1080.
16. **Kawaguchi, Y., J. J. Kovacs, A. McLaurin, J. M. Vance, A. Ito, and T. P. Yao.** 2003. The deacetylase HDAC6 regulates aggresome formation and cell viability in response to misfolded protein stress. Cell **115:**727–738.
17. **Kovacs, J. J., P. J. Murphy, S. Gaillard, X. Zhao, J. T. Wu, C. V. Nicchitta, M. Yoshida, D. O. Toft, W. B. Pratt, and T. P. Yao.** 2005. HDAC6 regulates Hsp90 acetylation and chaperone-dependent activation of glucocorticoid receptor. Mol. Cell **18:**601–607.
18. **Kozminski, K. G., D. R. Diener, and J. L. Rosenbaum.** 1993. High level expression of nonacetylatable alpha-tubulin in *Chlamydomonas reinhardtii*. Cell Motil. Cytoskelet. **25:**158–170.
19. **Kwon, S. H., Y. Zhang, and P. Matthias.** 2007. The deacetylase HDAC6 is a novel critical component of stress granules involved in the stress response. Genes Dev. **21:**3381–3394.
20. **Matsuyama, A., T. Shimazu, Y. Sumida, A. Saito, Y. Yoshimatsu, D. Seigneurin-Berny, H. Osada, Y. Komatsu, N. Nishino, S. Khochbin, S. Horinouchi, and M. Yoshida.** 2002. In vivo destabilization of dynamic microtubules by HDAC6-mediated deacetylation. EMBO J. **21:**6820–6831.
21. **Matthias, P., M. Yoshida, and S. Khochbin.** HDAC6: a new cellular stress surveillance factor. Cell Cycle, in press.
22. **North, B. J., B. L. Marshall, M. T. Borra, J. M. Denu, and E. Verdin.** 2003. The human Sir2 ortholog, SIRT2, is an NAD^+-dependent tubulin deacetylase. Mol. Cell **11:**437–444.
23. **Palazzo, A., B. Ackerman, and G. G. Gundersen.** 2003. Cell biology: tubulin acetylation and cell motility. Nature **421:**230.
24. **Palazzo, A. F., C. H. Eng, D. D. Schlaepfer, E. E. Marcantonio, and G. G. Gundersen.** 2004. Localized stabilization of microtubules by integrin- and FAK-facilitated Rho signaling. Science **303:**836–839.
25. **Rolink, A., U. Grawunder, T. H. Winkler, H. Karasuyama, and F. Melchers.** 1994. IL-2 receptor alpha chain (CD25, TAC) expression defines a crucial stage in pre-B cell development. Int. Immunol. **6:**1257–1264.
26. **Rual, J. F., K. Venkatesan, T. Hao, T. Hirozane-Kishikawa, A. Dricot, N. Li, G. F. Berriz, F. D. Gibbons, M. Dreze, N. Ayivi-Guedehoussou, N. Klitgord, C. Simon, M. Boxem, S. Milstein, J. Rosenberg, D. S. Goldberg, L. V. Zhang, S. L. Wong, G. Franklin, S. Li, J. S. Albala, J. Lim, C. Fraughton, E. Llamosas, S. Cevik, C. Bex, P. Lamesch, R. S. Sikorski, J. Vandenhaute, H. Y. Zoghbi, A. Smolyar, S. Bosak, R. Sequerra, L. Doucette-Stamm, M. E. Cusick, D. E. Hill, F. P. Roth, and M. Vidal.** 2005. Towards a proteome-scale map of the human protein-protein interaction network. Nature **437:**1173–1178.
27. **Schubart, K., S. Massa, D. Schubart, L. M. Corcoran, A. G. Rolink, and P. Matthias.** 2001. B cell development and immunoglobulin gene transcription in the absence of Oct-2 and OBF-1. Nat. Immunol. **2:**69–74.
28. **Seigneurin-Berny, D., A. Verdel, S. Curtet, C. Lemercier, J. Garin, S. Rousseaux, and S. Khochbin.** 2001. Identification of components of the murine histone deacetylase 6 complex: link between acetylation and ubiquitination signaling pathways. Mol. Cell. Biol. **21:**8035–8044.
29. **Serrador, J. M., J. R. Cabrero, D. Sancho, M. Mittelbrunn, A. Urzainqui, and F. Sanchez-Madrid.** 2004. HDAC6 deacetylase activity links the tubulin cytoskeleton with immune synapse organization. Immunity **20:**417–428.
30. **Tran, A. D., T. P. Marmo, A. A. Salam, S. Che, E. Finkelstein, R. Kabarriti, H. S. Xenias, R. Mazitschek, C. Hubbert, Y. Kawaguchi, M. P. Sheetz, T. P. Yao, and J. C. Bulinski.** 2007. HDAC6 deacetylation of tubulin modulates dynamics of cellular adhesions. J. Cell Sci. **120:**1469–1479.
31. **Valenzuela-Fernandez, A., S. Alvarez, M. Gordon-Alonso, M. Barrero, A. Ursa, J. R. Cabrero, G. Fernandez, S. Naranjo-Suarez, M. Yanez-Mo, J. M. Serrador, M. A. Munoz-Fernandez, and F. Sanchez-Madrid.** 2005. Histone deacetylase 6 regulates human immunodeficiency virus type 1 infection. Mol. Biol. Cell **16:**5445–5454.
32. **Vaquero, A., M. B. Scher, D. H. Lee, A. Sutton, H. L. Cheng, F. W. Alt, L. Serrano, R. Sternglanz, and D. Reinberg.** 2006. SirT2 is a histone deacetylase with preference for histone H4 Lys 16 during mitosis. Genes Dev. **20:**1256–1261.
33. **Verdel, A., S. Curtet, M. P. Brocard, S. Rousseaux, C. Lemercier, M. Yoshida, and S. Khochbin.** 2000. Active maintenance of mHDA2/mHDAC6 histone-deacetylase in the cytoplasm. Curr. Biol. **10:**747–749.
34. **Verdel, A., and S. Khochbin.** 1999. Identification of a new family of higher eukaryotic histone deacetylases. Coordinate expression of differentiation-dependent chromatin modifiers. J. Biol. Chem. **274:**2440–2445.
35. **Verdin, E., F. Dequiedt, and H. G. Kasler.** 2003. Class II histone deacetylases: versatile regulators. Trends Genet. **19:**286–293.
36. **Wang, S., Y. Yan-Neale, M. Zeremski, and D. Cohen.** 2004. Transcription regulation by histone deacetylases. Novartis Found. Symp. **259:**238–248, 285–288.
37. **Westendorf, J. J., S. K. Zaidi, J. E. Cascino, R. Kahler, A. J. van Wijnen, J. B. Lian, M. Yoshida, G. S. Stein, and X. Li.** 2002. Runx2 (Cbfa1, AML-3) interacts with histone deacetylase 6 and represses the $p21^{CIP1/WAF1}$ promoter. Mol. Cell. Biol. **22:**7982–7992.
38. **Westermann, S., and K. Weber.** 2003. Posttranslational modifications regulate microtubule function. Nat. Rev. Mol. Cell Biol. **4:**938–947.
39. **Yang, X. J., and S. Grégoire.** 2005. Class II histone deacetylases: from sequence to function, regulation, and clinical implication. Mol. Cell. Biol. **25:**2873–2884.
40. **Zhang, X., Z. Yuan, Y. Zhang, S. Yong, A. Salas-Burgos, J. Koomen, N. Olashaw, J. T. Parsons, X. J. Yang, S. R. Dent, T. P. Yao, W. S. Lane, and E. Seto.** 2007. HDAC6 modulates cell motility by altering the acetylation level of cortactin. Mol. Cell **27:**197–213.
41. **Zhang, Y., B. Gilquin, S. Khochbin, and P. Matthias.** 2006. Two catalytic domains are required for protein deacetylation. J. Biol. Chem. **281:**2401–2404.
42. **Zhang, Y., N. Li, C. Caron, G. Matthias, D. Hess, S. Khochbin, and P. Matthias.** 2003. HDAC-6 interacts with and deacetylates tubulin and microtubules in vivo. EMBO J. **22:**1168–1179.